9-15-2001

Effects of River Inputs into the Bay of Bengal

Stephan D. Howden
University of Southern Mississippi, stephan.howden@usm.edu

Raghu Murtugudde
University of Maryland

JOURNAL OF GEOPHYSICAL RESEARCH, VOL. 106, NO. C9, PAGES 19,825–19,843, SEPTEMBER 15, 2001

Effects of river inputs into the Bay of Bengal

Stephan D. Howden

Department of Marine Science, University of Southern Mississippi, Stennis Space Center, Mississippi

Raghu Murtugudde

Earth Systems Science Interdisiplinary Center, University of Maryland at College Park, College Park, Maryland

Abstract. The effect of river runoff in the Bay of Bengal is examined using a reduced gravity primitive equation ocean model coupled to an atmospheric boundary layer model. Model simulations are carried out by including river discharges as surface freshwater forcing at the mouths of the rivers. To assess the effect of river inputs on the dynamics and thermodynamics of the tropical Indian Ocean, parallel simulations are carried out by neglecting the river inputs. Additionally, another set of parallel runs without penetrative radiation loss through the mixed layer is carried out. The freshwater flux due to rivers results in lower salinities and shallower mixed layers, as expected. However, the influence of this additional freshwater flux into the bay is rather counterintuitive. With the inclusion of river discharges more heat is absorbed by the ocean, but sea surface temperatures are slightly cooler in the bay because of enhanced entrainment cooling of the shallower mixed layer, enhanced penetrative radiation, and an enhanced effect of latent heat loss on the temperature tendency. This is despite the greater latent heat loss when river input is neglected. Conversley, neglect of penetrative radiation results in a shallower but slightly warmer mixed layer with river input. River input and penetrative radiation each affect the mixed layer depths, the salinity and temperature structure, and currents in the Bay of Bengal, but they have a small effect on SST. Annual SST, averaged over the Bay of Bengal, is only 0.1°C colder with river input. Neglecting penetrative radiation in the river run results in an increase of only 0.2°C for the annual SST. The lack of persistence of a barrier layer in the bay helps regulate SST even in the presence of enhanced buoyancy forcing due to river input. Averaged over the bay, a barrier layer forms as mixed layer detrainment occurs, and the thermocline deepens just after the southwest monsoon and the northeast monsoon. The barrier layer is short-lived in each case it is eroded by mixing. The effect of riverine input in the bay is not confined to the surface waters. A pool of cold anomaly (-1°C) and fresher waters is centered near 100 m depth in the bay with riverine input. This cold pool beneath the mixed layer allows entrainment cooling of the mixed layer to be more effective, even though mass entrainment is lower relative to the case neglecting river input. The more diffuse thermocline in the bay is consistent with enhanced vertical mixing despite the large positive buoyancy forcing.

1. Introduction

The Bay of Bengal is the freshest region in the Indian Ocean by virtue of both direct monsoonal rainfall and by large riverine input. The onset of the summer monsoon rainfall occurs on the eastern side of the bay (near to the outflow of the Irrawaddy River) and over parts of Burma and Thailand and then spreads toward the northwest [*Ramage et al.*, 1972]. During the summer southwest monsoon (SWM), river runoff doubles the surface freshwater input (precipitation P minus evaporation E) into the bay to nearly $183\times10^{11}\mathrm{m}^3$ [*Varkey et al.*, 1996] (hereinafter referred to as VMS96). The surface salinity and density fields show marked variations both spatially and temporally as a result of the large freshwater inputs, highly variable monsoonal winds and associated upwelling/downwelling, and advection from the west and south of high-salinity water masses [*VMS96*]. *Sewell* [1929] showed large meridional gradients of sea surface salinity (SSS) in the bay during the post-summer monsoon period (September-November when river input by the Ganges and Irrawady

Paper number 2000JC000656.
0148-0227/01/2000JC000656$09.00

are large) with weaker meridional gradients in March–April. SSS climatology [*Levitus, et al.,* 1994] shows strong meridional gradients on the western side of the bay developing in June-September, with salinity dropping by more than 6 psu from the mouth of the bay to about 15°N, and the gradient decreasing in subsequent months. On the eastern side of the bay the *Levitus* [1994] climatology shows the meridional gradient building from June until December with maximum changes of over 5 psu from the mouth of the bay to the Irrawady outflow region. In addition to the large freshwater forcing, with phase lags between precipitation and river input, the circulation of the bay undergoes dramatic changes due to strong seasonal variations in upwelling/downwelling, locally generated Rossby and coastal Kelvin waves, and Ekman flow all associated with the monsoonal winds. Additionally, nonlocal forcing results in Rossby and coastal Kelvin wave propagation into the bay [*Potemra et al.,* 1991; [*Yu et al.,* 1991], though *McCreary et al.,* [1993] found the modeled coastal currents to be affected more by wind stress forcing within the bay, except on the eastern side.

The significance of the salinity variability of the bay is not confined within its basin. Observational studies have linked the advection by the East Indian Coastal Current (EICC) of fresh bay water into the southeast corner of the Arabian Sea (AS) and then to the formation of a barrier layer (*Godfrey and Lindstrom*, 1989; *Lukas and Lindstrom*, 1991) and, subsequently, a surface warm pool (Rao and Sivakumar, 1999). The warm pool in the southeast AS forms completely independently of the migration of the thermal equator (TE) and associated Intertropical Convergence Zone (ITCZ), and it has been implicated in the formation of the monsoon onset vortex (*Rao and Sivakumar*, 1999) that is nearly always associated with the onset of the summer monsoon on the Indian subcontinent. *Shenoi et al.*, [1999] found the annual cycle of SST in this region leads that of surrounding waters and peaks in April well before the migration of the TE into the region.

Modeling studies have shown that fresh water from the bay also flows south along the eastern boundary during the SWM (*Han* 1999, hereinafter referred to as Han99; *Han and McCreary*, 2001). Han99 showed that once this water reaches the equator, some of it is advected westward by the equatorial flow, and some continues southward until it is advected westward by the South Equatorial Current, where, subsequently, a portion is advected northward by the East African Coastal Current and Somalia Current during the SWM, and the remainder flows out of the Indian Ocean at the western boundary. The effect of this freshwater advection is to lower the SSS in the equatorial and southern tropical Indian Ocean by 0.1-1 psu.

Han99 [see also *Han and McCreary*, 2001; *Han, et al.,* 2001] did an extensive modeling study of the influence of salinity on the dynamics and thermodynamics of the Indian Ocean. As part of that study, the role of river input in the Bay of Bengal in affecting the dynamics and thermodynamics of the Indian Ocean was done. Interestingly, significant changes in SST in the bay only occur in very localized regions: warming in the NW corner during the summer monsoon and cooling in the NW corner and the southeastern bay during March. The other regions with appreciable SST differences are along the equator and off of the Somali coast. This weak effect on SST occurs despite large differences in salinity, both surface and subsurface. Han99 used a 4.5-layer model with specified heat fluxes and winds. The present study extends the examination of the effects of river input in the Bay of Bengal in several important respects. First, the Indian Ocean is modeled with a 20-layer model that allows a more realistic barrier layer to form (i.e., multiple layers below the mixed layer may have nearly identical temperature but differing salinity). Second, the ocean model is coupled to an advective atmospheric mixed layer (AML) model, which allows interactive heat fluxes and hence allows more freedom for SST adjustment. Third, daily rather than monthly wind forcing is used.

2. Approach

Model simulations are carried out by including river discharges as surface freshwater forcing at the mouth of rivers. To assess the effect of river inputs on the dynamics and thermodynamics of the tropical Indian Ocean, parallel simulations are carried out by neglecting river inputs. Additionally, the effects of penetrative radiation are assessed by running parallel runs with and without penetrative radiation.

2.1. Model Description

The ocean general circulation model (OGCM) is the reduced gravity, primitive equation, sigma coordinate model of *Gent and Cane* [1990] with variable salinity and an embedded hybrid mixing scheme of *Chen et al.* [1994]. Surface heat fluxes are computed by coupling the OGCM to an advective AML model [*Seager et al.,* 1995]. *Seager et al.* [1995] describe how such a scheme allows true simulation of SST, rather than building in the answer as imposing air temperature and humidity does. *Murtugudde et al.* [1996] showed the improvements in simulations of tropical SST and associated feedbacks on model dynamics/thermodynamics using this model. The OGCM has a variable depth mixed layer and 19 layers below according to a sigma coordinate. The mixed layer depth (MLD) and the thickness of the last sigma layer are computed prognostically, and the remaining layers are computed diagnostically such that the ratio of each sigma layer to the total depth below the mixed layer is held to its prescribed value. The hybrid vertical mixing scheme [*Chen et al.,* 1994] allows for relating the atmospheric forcing to the mixed layer entrainment/detrainment through a traditional bulk mixed layer model [*Kraus and Turner*, 1967], shear flow instability through the dynamic instability model of *Price et al.* [1986], and an instantaneous

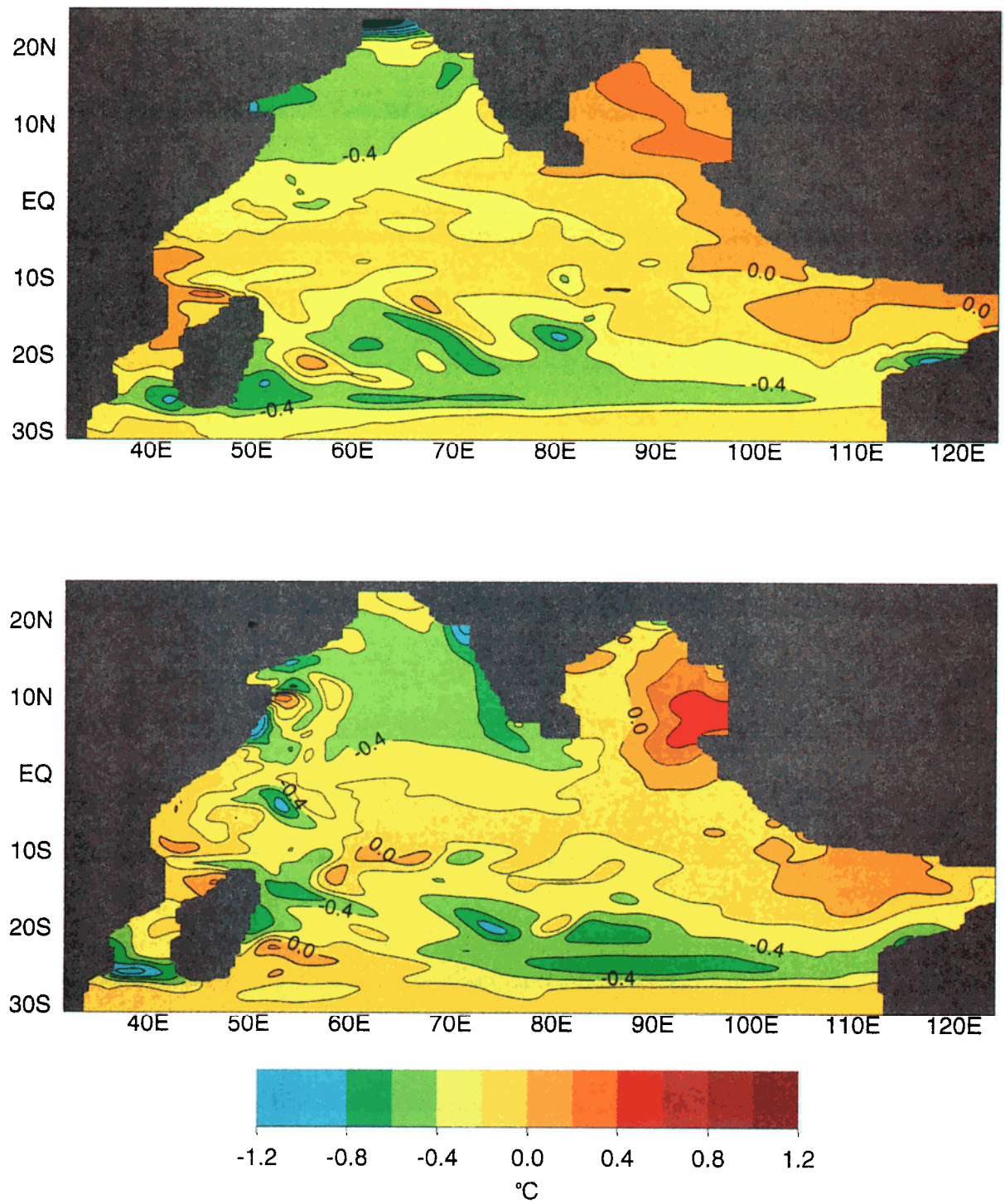

Plate 1. SST differences over entire model domain between (top) model forced by monthly and (bottom) model forced by daily winds. Both runs include river input.

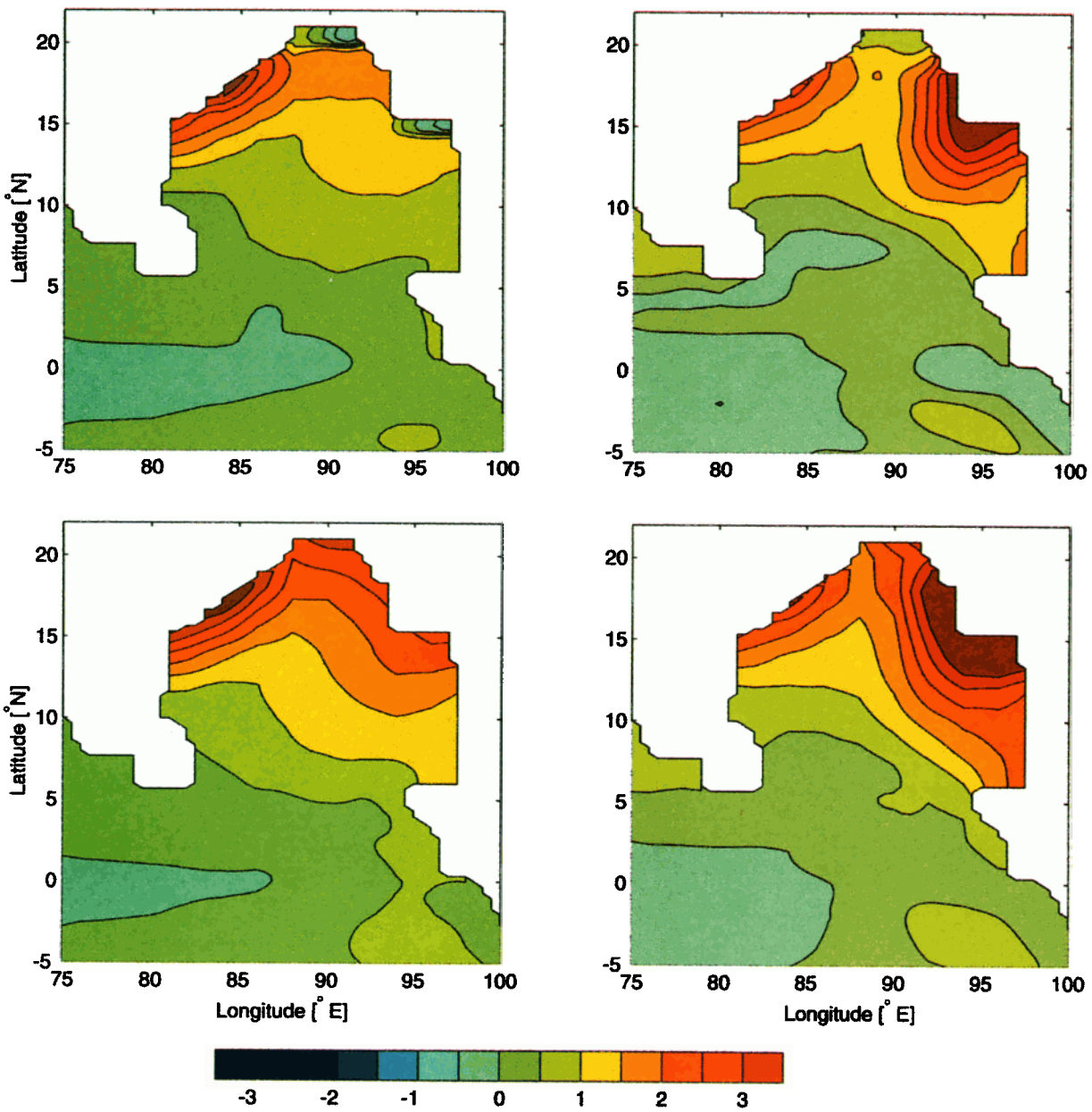

Plate 2. Model SSS minus *Levitus* [1994] SSS during (left) summer and (right) winter monsoons: (top) the differences between R1 and Levitus climatology and (bottom) the differences between C1 and Levitus climatology. The countour interval is 0.5 psu. The dashed lines are negative contours.

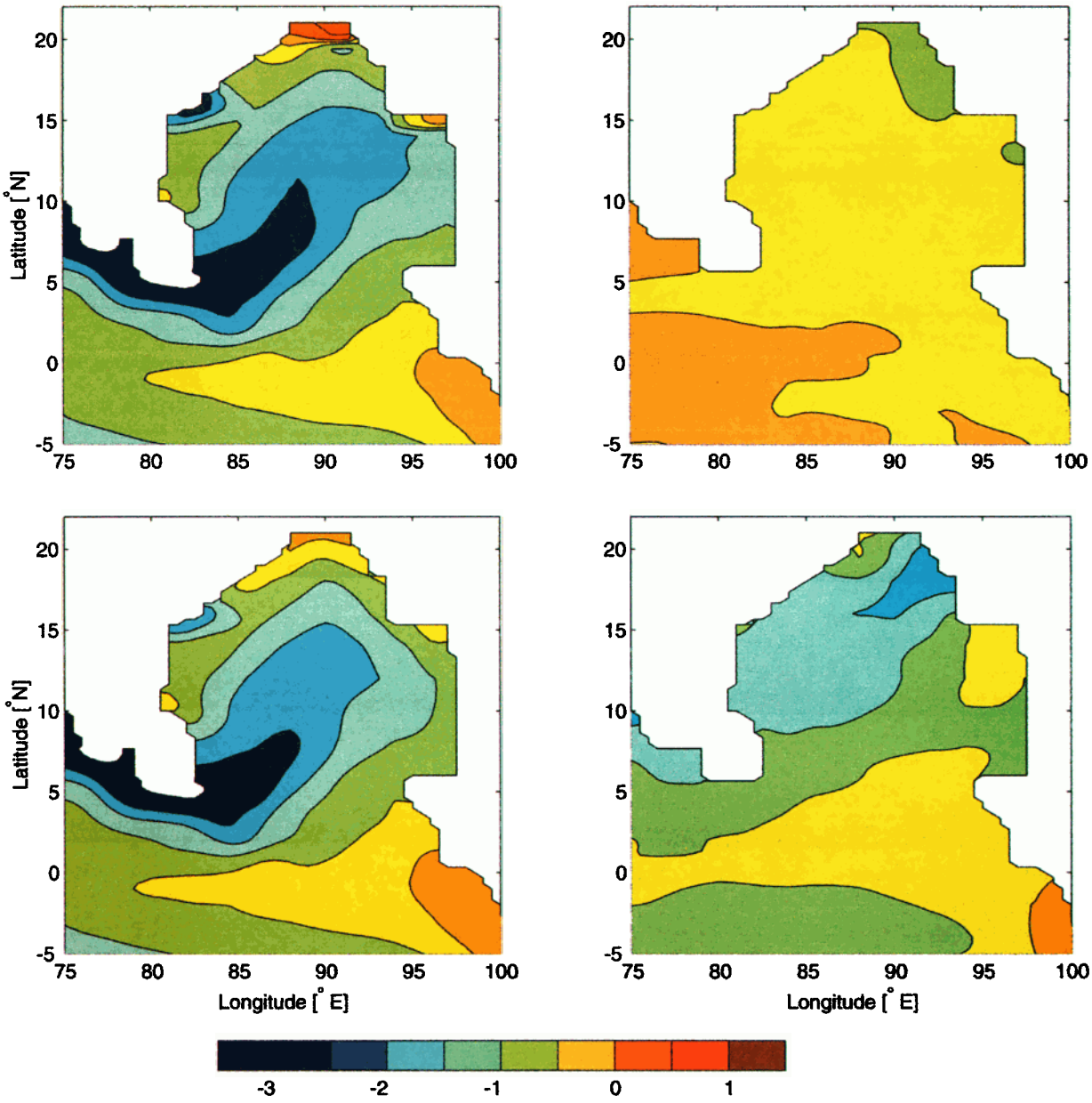

Plate 3. Model SST minus *Levitus* [1994] SST during (left) summer and (right) winter monsoons: (top) the differences between R1 and Levitus climatology and (bottom) the differences between C1 and Levitus climatology. The countour interval is 0.5°C. The dashed lines are negative contours.

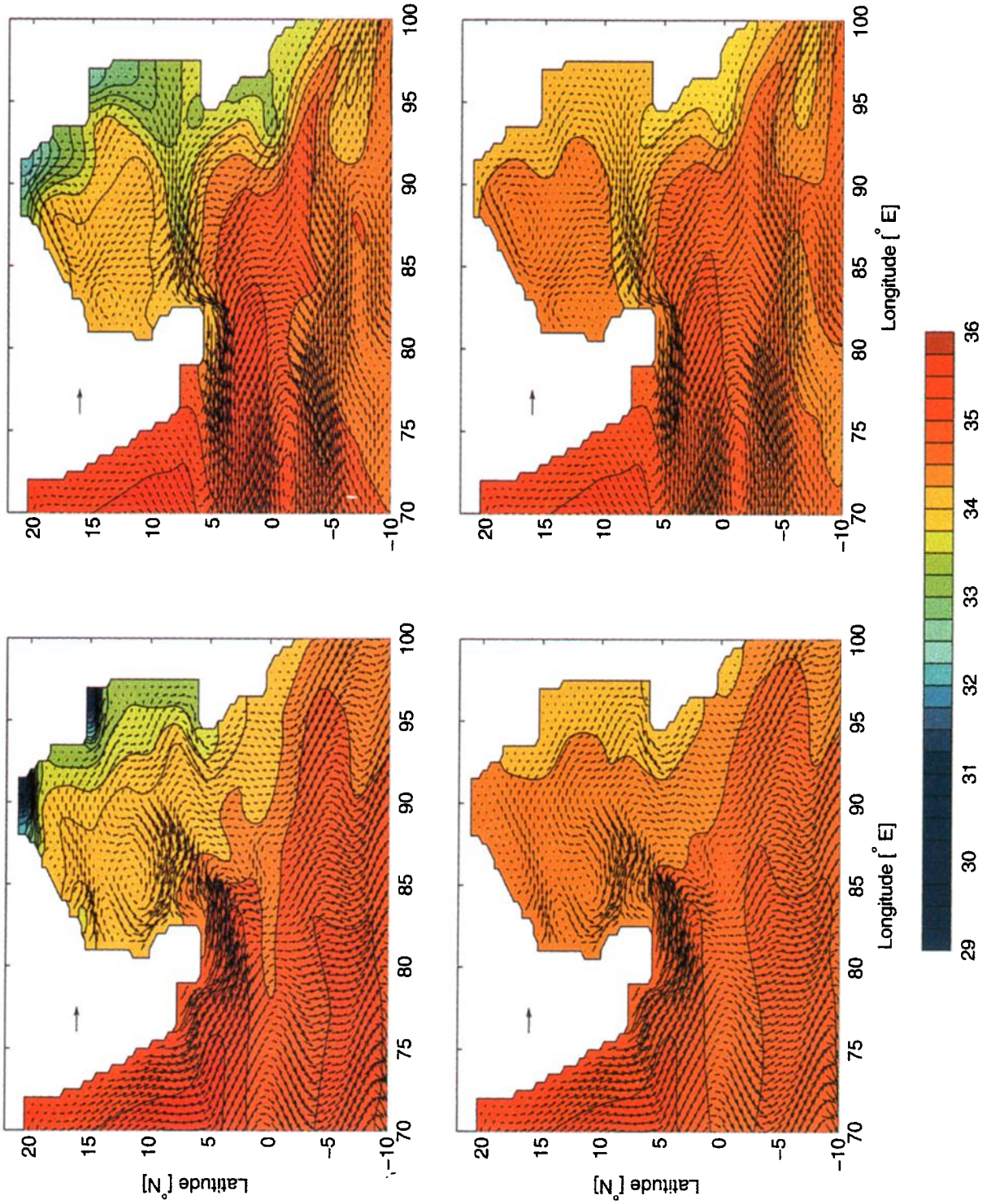

Plate 4. SSS and surface current vectors: (left) SWM average, (right) NEM average, (top) run R1 and (bottom) run C1.

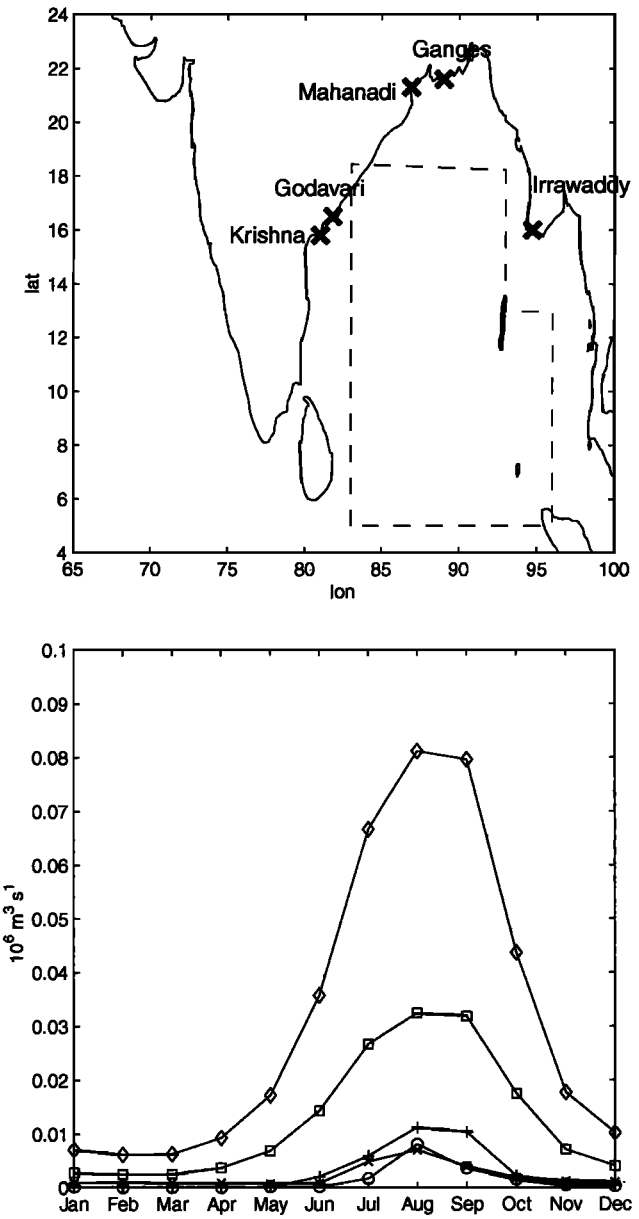

Figure 1. Climatologies of major river inflow into the Bay of Bengal: (top) locations of river outflows and the bounding box for Bay of Bengal averaging and (bottom) river inflow climatologies from. Diamonds, squares, pluses,crosses, and circles denote the Ganges-Bramuputra, the Irrawady, the Godavari, the Mahanadi, and the Krishna river outflows, respectively.

adjustment to simulate high-frequency convection in the water column.

Complete hydrology has been added to the model with freshwater forcing treated as a natural boundary condition [*Huang*, 1993]. The buoyancy is computed from salinity and temperature using the United Nations Educational, Scientific, and Cultural Organization's (UNESCO) equation of state.

Surface latent and sensible heat fluxes are computed using the ocean model SST, the imposed winds, and air temperature and humidity from the AML. Longwave radiative heat loss from the surface is computed using a standard bulk formula and observed cloud cover [*Seager and Blumenthal*, 1994]. Solar radiative forcing is taken from the Earth Radiation Budget Experiment satellite data of *Li and Leighton* [1993].

Since evaporation is computed by the AML with modeled SST, only precipitation P data are required for freshwater forcing over the ocean. P was obtained from *Oberhuber's* [1988] atlas. Monthly river volume input values were taken from UNESCO reports. The five major rivers that empty into the Bay of Bengal are the Krishna, the Godavari, the Mahanadi, the Ganges, and the Irrawady (Figure 1). Because of the lack of data about the Irrawady, the river input was taken to be 40% of the Ganges input which is what Han99 reported from S. Shetye (personal communication, 1996). The river inputs are included in the model as surface freshwater forcing in the nearest $2° \times 2°$ grid points surrounding the discharge locations. Table 1 lists the fields used for model boundary conditions, initialization, and forcing.

Five different model runs were done. The control run (C1) does not include river input. R1 is identical to the control run except that river input is included. Runs C1 and R1 were duplicated in runs C2 and R2, respectively, except that penetrative short wave radiation was neglected. The final run (R3) is the same as R1 except that monthly wind forcing was used. This model run was performed to examine the differences between monthly and daily climatological wind forcing.

3. Results

3.1. Monthly Versus Daily Wind Forcing

The effect of using daily versus monthly climatological wind forcing is seen in Plate 1. Plate 1 shows SST from monthly wind forcing minus that from daily wind forcing averaged over the period (top) December-February and (bottom) July-September for the entire model domain. Within the Bay of Bengal the run with monthly forcing is consistently warmer than that with daily forcing, with the exception of the Ganges outflow region during the northeast monsoon. The cooler SST with daily forcing is consistent with more vigorous vertical mixing associated with higher-frequency forcing. Indeed, the SST difference is even greater during the SWM when the main thermocline is shallowest (as will be shown in section 3.4).

3.2. Comparison With *Levitus* [1994] Surface Climatology

Throughout most of the year the model runs are fresher than *Levitus* [1994] climatology (references to climatology hereafter refer to this climatology) in the bay. However, between the NEM and the SWM the model runs are generally more saline than climatology in the bay. Overall, runs C2 and R2 have larger differences (both positive and negative) from climatology. As

Table 1. Data for Indian Ocean Model

Parameter	Data
Domain	32°-124°E×30°S–26°N (T_b = 9°C, S_b = 35 psu)
Horizontal resolution	X: 2/3° uniform
	Y: 1/3° uniform
Vertical resolution	hybrid mixed layer + 19 σ layers with
	$\sigma = 4 \times 2.5/350,\ 4 \times 5/350,\ 4 \times 10/350,\ 2 \times\ 15/350,$
	$2 \times 25/350,\ 2 \times 50/350,\ 2 \times 75/350$
Wind stresses	NCEP daily averaged 6 hourly winds
	NCEP monthly averaged 6 hourly winds
Initial conditions	Initial stratification derived from *Levitus* [1994]
Boundary conditions	no-slip and no-heat flux conditions at
	lateral boundaries
	relaxation to *Levitus* [1994] climatology
	25°–30°S
Mixed layer	wind-mixing coefficient, cm=1.25
	Buoyancy coefficient, cn=0.17
	Maximum depth, max=125 m
	Minimum depth, min=10 m
Spin-up time	20 years with twenty-first year used for differences

expected, the river runs are closer to climatology than those without river input. Plate 2 illustrates the improvement of river input for simulating salinity during the summer and winter monsoons. Plate 2 shows model SSS minus climatological SSS. Plate 2 (left) shows the differences averaged during the SWM months of June, July, and August, Plate 2 (right) shows the differences averaged during the winter NEM months of December, January, and February. During the SWM the neglect of river input results in salinities higher than climatology everywhere in the bay, with differences of more than 4 psu. With river input the regions near the mouths of the Ganges and Irrawaddy Rivers are fresher than climatology; while nearly everywhere else, the absolute differences from climatology are reduced. Similar improvement occurs during the NEM period.

SST tend to be colder than climatology and have similar patterns regardless of river input (Plate 3) and q_{pen} (not shown). Exceptions occur close to the outflow regions of the Ganges and Irrawady during the SWM where SST is warmer than climatology with river input. SSTs are closest to the climatology during the NEM with river input. In that case, SST differences are <0.25°C throughout most of the bay.

3.3. Monsoonal Circulation and Hydrography

Plate 4 shows the SSS and velocity fields averaged over the NEM and SWM for runs C1 and R1. As was shown indirectly in Plate 2, the SSS fields are quite different with and without river input: surface salinity gradients are much larger with river input. During the summer monsoon, SSS with river input is up to 4.2 psu fresher, though a typical range in the interior of the bay is between 0.5 and 1.0 psu. Circulation features are very similar with and without river input, with the biggest differences occurring during the SWM at the edges of the freshwater pools at the Ganges and Irrawaddy outflow regions. Eastward flowing jets are associated with the fresh pools in these regions. Since these pools are fresh and warm, geostrophy would create a westward flowing current. The much thinner MLD results in a stronger eastward Ekman flow during the SWM. The river run has a stronger cyclone at roughly 10°N, 85°E and, more importantly, a weaker SWM current, bringing the saline AS waters into the bay. The deeper MLD just south of India with river input (Plate 5) is primarily responsible for the weaker SWM current as the Ekman flow is distributed over a thicker layer (geostrophic flow differences are generally <1 cm s^{-1} at 80°E). The stronger cyclone can be due to two factors. The run with river input does have fresher water along the east coast of India (Plates 2 and 4), raising the sea surface height there, and the main thermocline has a greater tilt down toward the east-northeast with river input (Plate 5).

During the NEM the lower-salinity waters from the bay are advected into the southeast AS by the westward flowing North Equatorial Current (NEC). It is this flow, made fresher by the waters of the EICC, that *Rao and Sivakumar* [1999] hypothesized creates a barrier layer in the southeastern AS warm pool region and is partially responsible for the warm pool creation. In the river run the NEC is stronger, with geostrophic flow up to 5 cm s^{-1} faster at 80°E. The fresher water along the southern coast of India is responsible for a higher sea level and hence a stronger meridional gradient in sea surface height.

As pointed out in section 1 Han99 and *Han and McCreary* [2001] showed that freshwater from the bay is advected southward along the eastern boundary during the SWM, with some making its way south of the equator. This is evident in Plate 4 where salinity is reduced along the eastern boundary all the way to 10°S with river input.

Plate 6 shows the surface salinity and currents for runs C2 and R2. Without q_{pen} the extra buoyancy forcing of the mixed layer causes the SSS to be much fresher with river input. The MLD is thinner without q_{pen}, and surface currents are intensified as Ekman flows are confined to a thinner layer and salinity gradients become larger.

Plate 5 shows differences during the SWM and the NEM between the model runs C1 and R1 of ML temperature (SST), MLD, barrier layer thickness (BLT), and depth of the 20° isotherm (Z_{20}, a proxy for the depth of the main thermocline). (Following a criteria set by *Sprintall and Tomczak* [1992], the BLT is computed from the model output by determining to what depth the temperatures are within 0.5°C of the ML temperature.) During the SWM most of the bay is cooler with river input (Plate 5a) with the most notable exceptions being at the grid points where the Ganges and Irrawaddy input is directed. During the NEM, nearly the entire bay is cooler with river input (Plate 5b), and most of the bay north of about 13°N is more than 0.4°C cooler. This contrasts with Han99 and *Han et al.* [2001], who showed large parts of the bay warmer (~0.2°C) with river input. However, in the run without q_{pen} (not shown), SST is actually slightly warmer with river input. The SST at the Krishna and Godavari outflow region is also slightly warmer with river input during the SWM. Again, Han99 and *Han et al.* [2001] showed a very different pattern of summertime SST with a large region in the northwest corner being warmer with river input. In section 3.5 the ML heat budget is examined to help explain these results. The MLD exhibits the largest differences in the north and northeastern parts of the bay (Plates 5c and 5d). During the SWM, MLDs near the Ganges and Irrawaddy rivers are over 40 m shallower with river input, as the buoyant river input suppresses entrainment. During the NEM the ML is shallower in the east and north with river input. During the SWM the barrier layer is very thin in both runs, and differences are near zero except right at the river outflows (Plate 5e). During the NEM, however, Plate 5f shows that BLT is smaller over most of the bay, except near the Ganges and Irrawaddy outflow regions where the BL is thicker with river input. Plates 5g and 5h illustrate that the main thermocline is 5-10 m shallower with river input over much of the bay during both the NEM and SWM. Since wind forcing and Ekman pumping are identical, these differences must be due to differences in mixing, subduction, or stratification. In the latter process an increase in density contrast between the thermocline and the upper waters, as might be expected with a surface freshwater input, will cause the thermocline to shoal.

The salinity signal due to river input is not confined to the surface layer. Plate 7 shows SWM- and NEM-averaged depth meridional sections of salinity along 90°E. A low-salinity plume extends from the head of the bay down toward the equator. The structure of this low-salinity plume, which is absent without river input, is similar to that shown in vertical sections in VMS96 and in recent sections taken during World Ocean Circulation Experiment and the Bay of Bengal Monsoon Field Experiment (BOBMEX) [P. Hacker, personal communication, 2000]. The 34 psu isohaline extends down to between 100 and 125 m depth in the northern part of the bay, and it surfaces near 11°N during the SWM. This compares with a late May section along 88°E during BOBMEX, which shows the same isohaline down to about the same depth and surfacing near 12°N. Another section taken during the SWM near 91°E (VMS96) shows the 34 psu isohaline down to about 75 m depth and surfacing near 9°N.

The modeled low-salinity plume also compares favorably with sections taken during the NEM. VMS96 show a section taken along 88°E that has the 34 psu isohaline at about 80-100 m depth and surfacing near 6°N. The modeled plume shows the 34 psu isohaline surfacing at about 12°N and then shoaling at 9°N and surfacing again at about 5°N. The higher-salinity waters centered at about 10°N in the modeled plume also appears in the observed section.

When q_{pen} is ignored (Plates 7e, 7f, 7g and 7h) the low-salinity plume is fresher and extends deeper in the water column. The 34 psu isohaline extends down near 175 m in the SWM and surfaces near the equator, and it extends slightly deeper during the NEM.

The salinity and horizontal velocity fields at 100 m depth are shown in Plate 8. During both the SWM and the NEM, low-salinity bay waters are advected in westward currents in the southern portion of the bay, though during the SWM some of these waters are recirculated in an anticyclonic eddy. Like at the surface, the overall characteristics of the flow are similar regardless of river input.

Figure 2 shows zonal depth cross sections of meridional flow along 7°N during the SWM and the NEM for run R1. The patterns of the flow are similar without river input. During the SWM, there is northward flow along the western side of the bay with maximum flow centered at about 50 m depth. Another northward flowing current occurs at about 87°E and is confined to the upper 100 m. There is also northward flow along the eastern boundary below 225 m. When river input is neglected, the northward flow into the bay at the surface is enhanced: The deeper ML creates a weaker southward component of Ekman flow, countering the northward geostrophic flow. Below the surface, however, the northward flow is enhanced with river input. The geostrophic surface flow is nearly identical on the western boundary so this difference is due to changes in stratification below the ML. The surface flow out of the bay along the eastern boundary is also enhanced when river input is neglected (C1), though the subsurface southward flow is stronger with river input. From about 92° to 95°E the northward geostrophic flow is about 2.5 cm s^{-1} faster with river input. During the

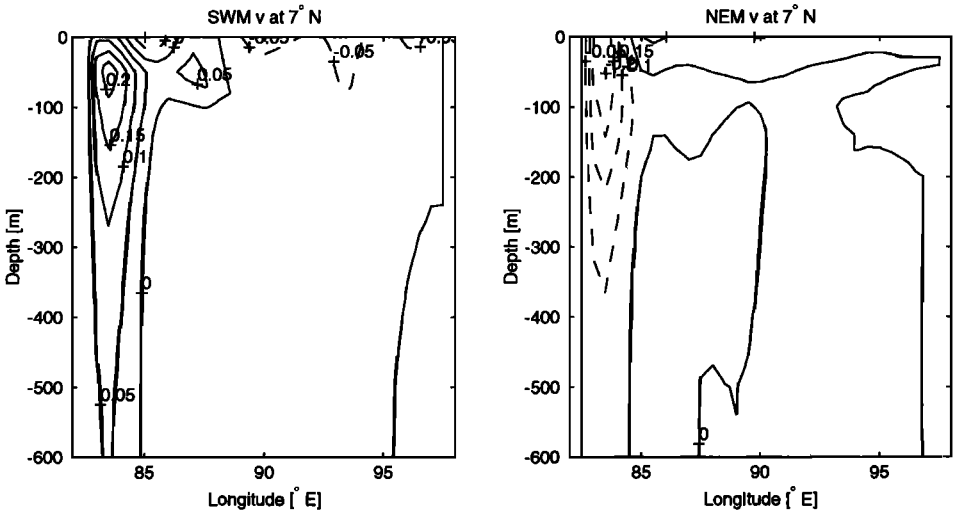

Figure 2. Meridional velocity along 7°N averaged over the (left) SWM and (right) NEM for run R1.

NEM the most prominent feature is the southward flow along the western boundary. This flow is more surface intensified than the northward flow during the SWM. When river input is neglected, this southward flow out of the bay is weaker. The southward geostrophic flow is more intense with river input as fresh water along the western boundary raises sea level. This is consistent with Han99 and *Han et al.* [2001] who showed that river input creates a stronger cross-shore pressure gradient along the east coast of India.

Figure 3 shows differences between runs C1 and R1 of vertical profiles averaged from 5° and 18°N, along 90°E. The differences in temperature between the runs (Figure 3a) are more evident here than in Plate 7. Although the SST differences are small (~0.2°C), run C1 is nearly 1°C warmer near 100 m depth during both the SWM and the NEM. Between about 200 and 300 m, run C1 is about 0.25° colder during the SWM and about 0.2°C colder during the NEM. The low-salinity plume is very evident in Figure 3b. The density difference profile (Figure 3) shows that the control run is denser within the upper 80 m (the lower salinity affects density more than the cooler temperatures). From 80 to 125 m the riverine run is more dense, while the opposite holds again from 125 to about 300 m.

The low-salinity plume and the cooler waters in the upper 200 m are consistent with enhanced vertical mixing in the riverine run. Plate4 shows that surface currents are very strong at the edge of the fresh pools at the river outflows. Presumably, strong vertical shears in the region will become unstable, and vigorous vertical mixing can occur. To some extent the temperature fields adjust to counter the density changes caused by the freshwater river input: the low-salinity plume is coincident with a cold plume (i.e., in the temperature difference field), except right at the surface where the river outflow occurs. The more diffuse thermocline with positive anomalies below and negative anomalies above the main thermocline is consistent with enhanced vertical mixing.

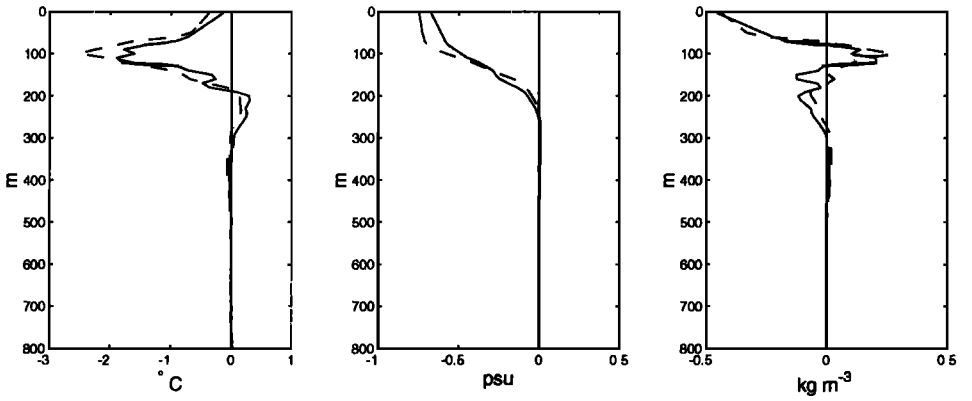

Figure 3. (a) Temperature, (b) salinity, and (c) density profile differences averaged between 5° and 18°N, along 90°E. The profiles are for the differences between R1 and C1. Solid lines are for the SWM, and dashed lines are for the NEM.

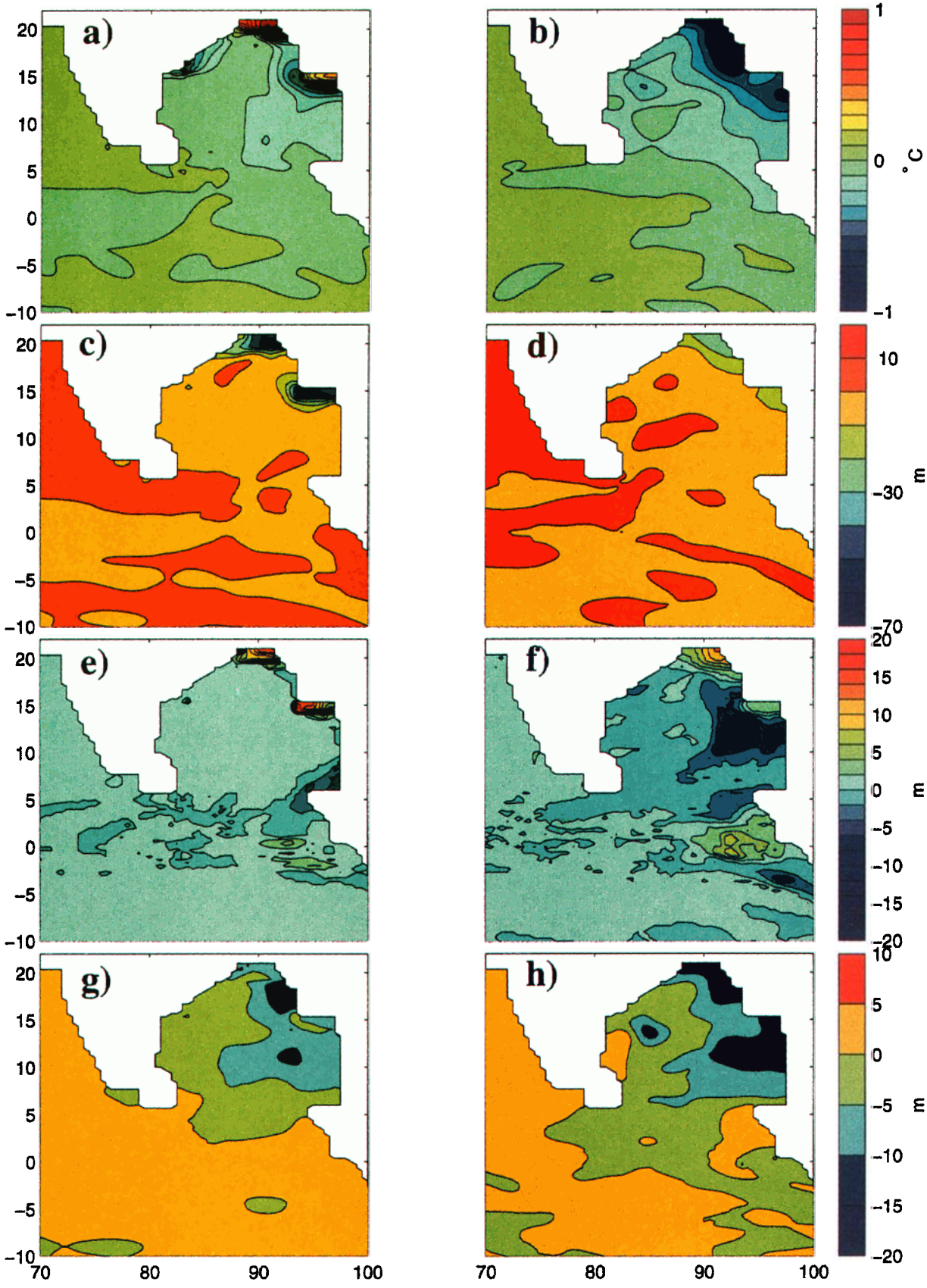

Plate 5. Differences between R1 and C1: fields averaged over (left) SWM and (right) NEM. (a) and (b) SST (contour interval=0.1°C), (c) and (d) MLD (c.i.= 5 m), (e) and (f) BLT (c.i.= 2m), (g) and (h) $Z20$ (c.i.=5 m)

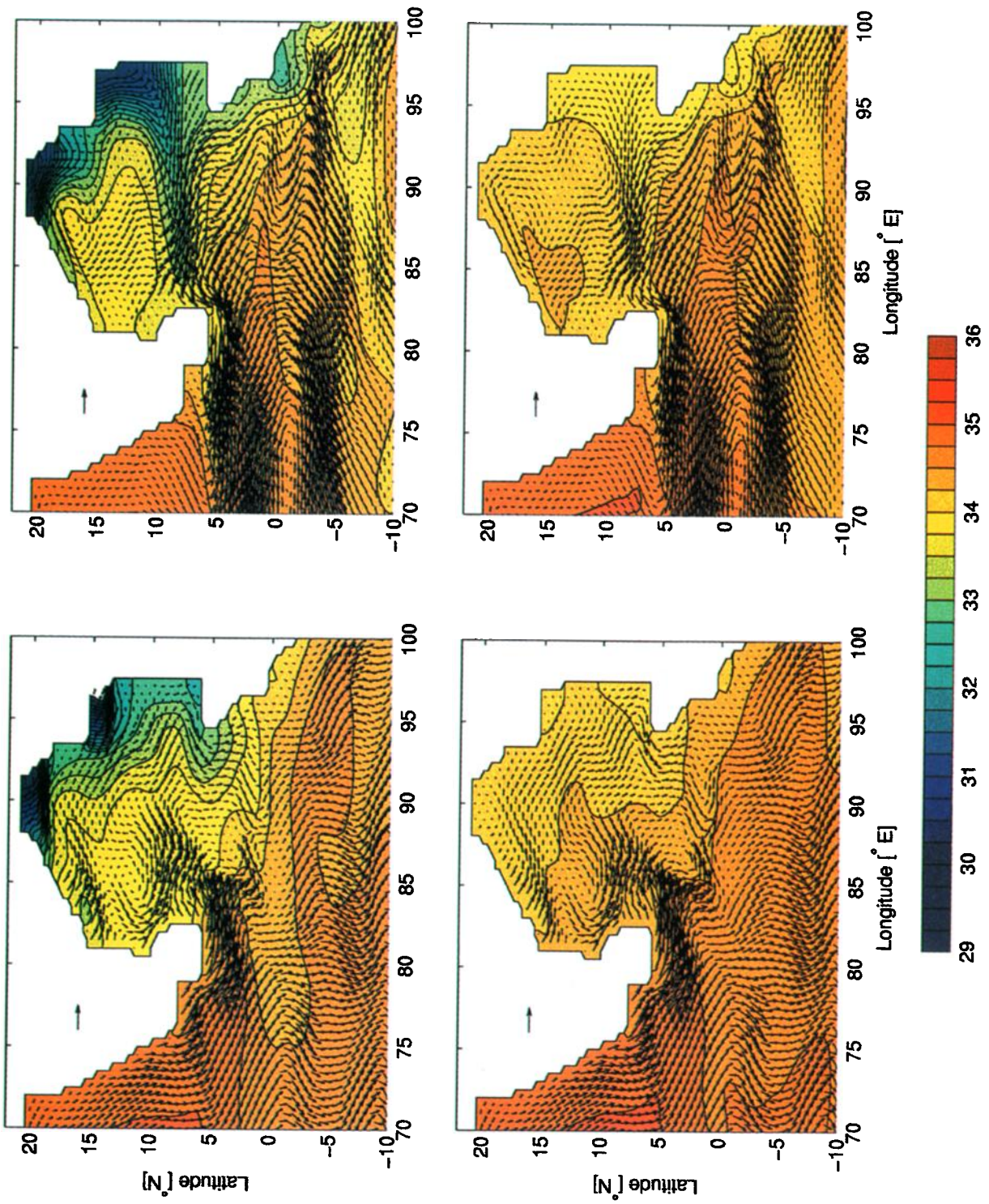

Plate 6. Similar to Plate 4 except q_{pen} is absent (i.e., runs C2 and R2).

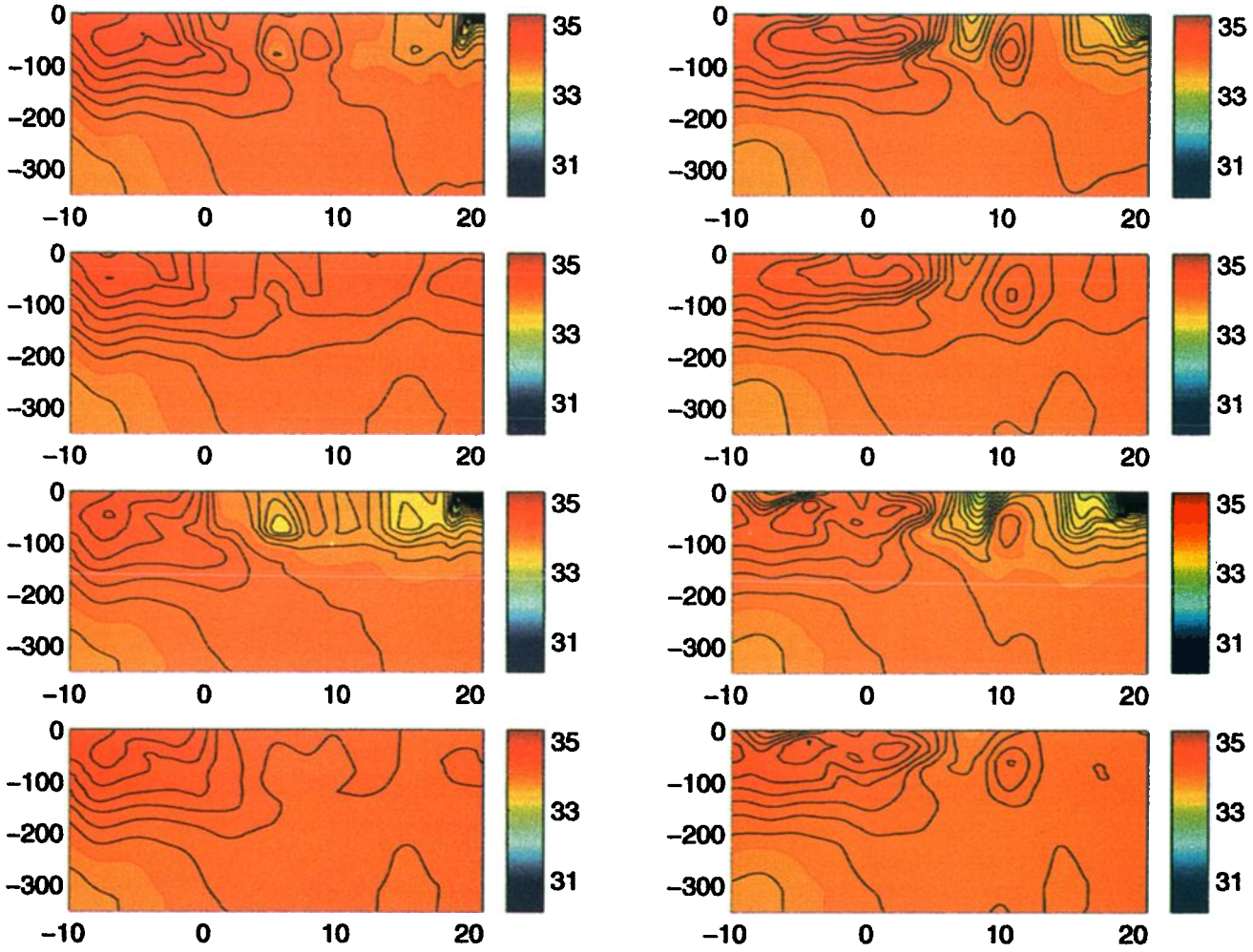

Plate 7. Vertical meridional sections of salinity at 90°E, averaged over the (left) SWM and (right) NEM: (a) and (b) run R1, (c) and (d) run C1, (e) and (f) run R2, and (g) and (h) run C2. The 34 psu isohaline is contoured in red. The contour interval is 0.1 psu.

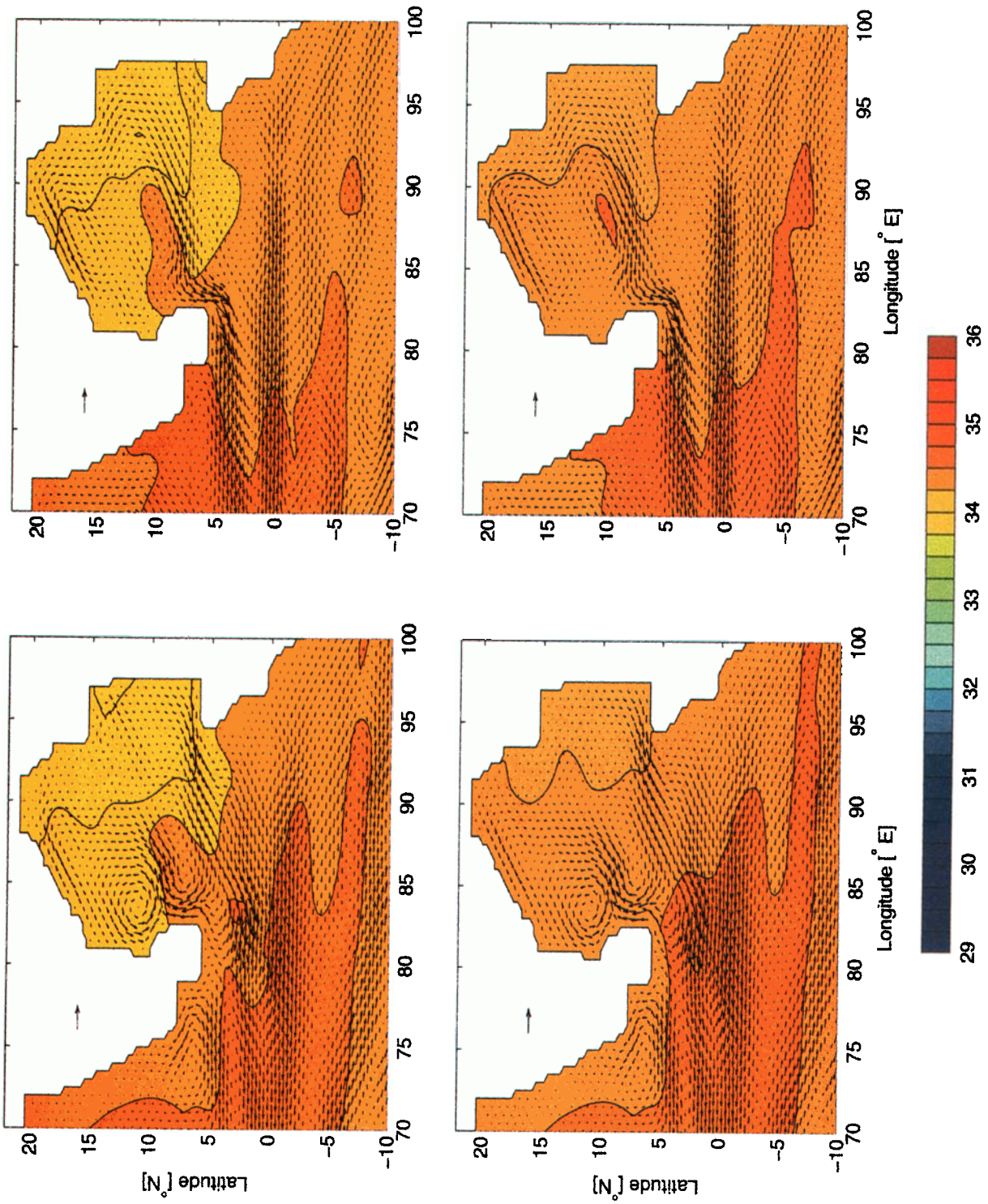

Plate 8. Same as Plate 4, except at 100 m depth. Fields are interpolated to 100 m from sigma levels.

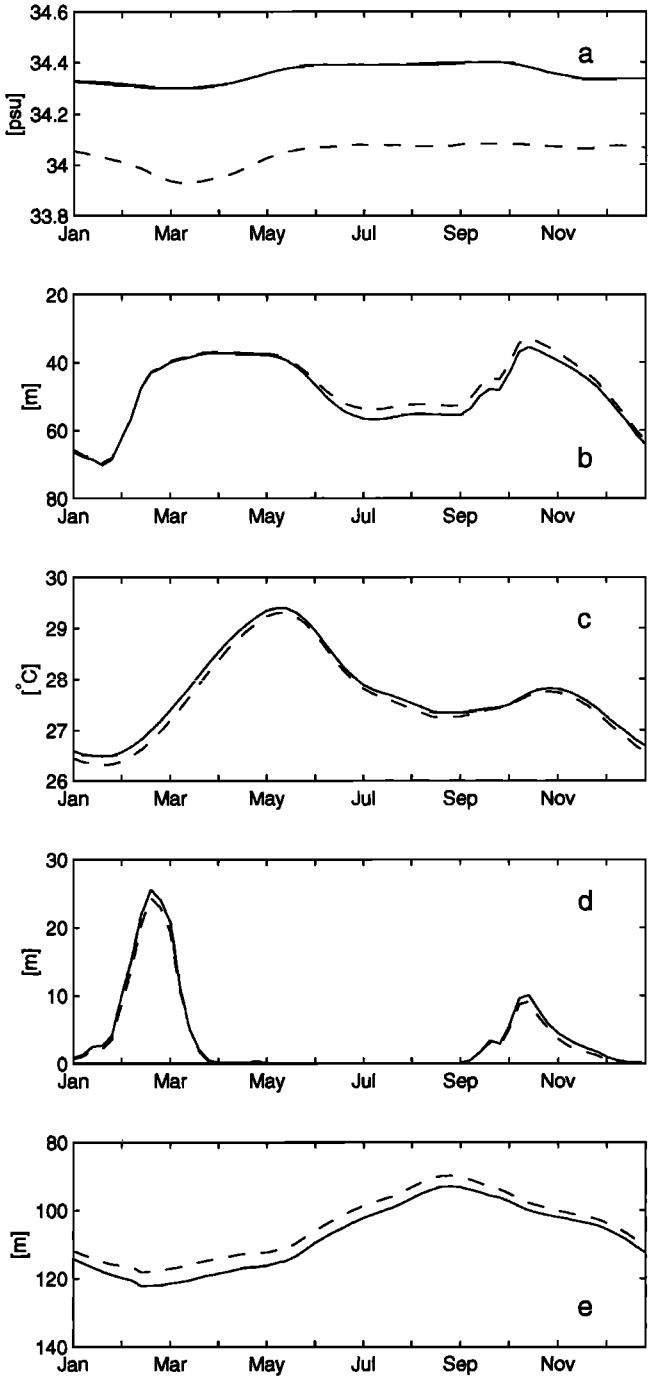

Figure 4. ML and BL properties averaged over the Bay of Bengal interior for runs R1 and C1 (see Figure 1 for averaging area): (a) ML salinity (SSS), (b) MLD, (c) ML temperature (SST), (d) BLT and (e) $Z20$. Properties from river input run (R1) are plotted with dashed lines.

3.4. Bay of Bengal Averaged Time Series

Figure 4 shows time series of ML properties, BL depth, and main thermocline depth (depth of the 20°C isotherm) averaged over the interior of the bay in the L-shaped region in Figure 1. The region is chosen to look for large-scale SST changes that would be important for forcing the atmosphere and, at the same time, to avoid the area of direct river input where the model has to adjust to the freshwater input. The annual cycle of the ML and BL properties have not previously been well characterized from either modeling or observational studies. The ML properties exhibit prominent semiannual variability, which is characteristic in the monsoon region, while the main thermocline exhibits a mostly annual variability. The main thermocline variability is set by both the local forcing and the remotely generated Rossby waves [e.g., *Potemra et al.*, 1991; *Yu et al.*, 1991]. This result agrees qualitatively with the annual cycle of the 20°C isotherm along 85°E (north of 5°N) in the *Levitus* [1984] climatology shown by *Vinayachandran and Yamagata* [1998]. As expected, the ML is fresher with river input (Figure 4a) with a difference of ~0.3 psu on the annual average. Variations of ML salinity (SSS) within the individual runs is much less than this mean difference with a range of 0.15 psu with rivers and 0.10 psu without rivers. When q_{pen} is neglected the annual ML SSS is another 0.3 psu fresher with river input (not shown) as a shallower and more buoyant ML forms.

The ML is shallowest (Figure 4b) during the periods of light wind between the NEM and the SWM (March-May and October-November). The shallowest (~33 m) period is in October for both model runs. The onset of the monsoonal winds (May-June for the SWM and November for the NEM) signals the beginning of ML deepening, with the deepest ML occurring in January. The greatest difference (~3.2 m) in MLD occurs in August. Annually, the MLD is 1.5 m shallower with river input which is not unexpected since it is also fresher. When q_{pen} is neglected, and all shortwave radiation is dumped into the ML, on the annual average the ML is ~13 m thinner. Thus it is important to include q_{pen}.

ML temperature (SST, Figure 4c) increases from January to May as solar radiation increases and the winds remain light. SST then drops at the onset of the SWM and continues to decrease until the end of the SWM in August. It then rises slightly before the NEM winds begin in November, after which it drops to its lowest temperatures (26.5°C without rivers and 26.3°C with rivers) in January. Interestingly, the thinner and more buoyant ML with river input is always colder than that without river input. The largest difference occurs in January when the ML is 0.2°C colder with river input. Annually, the difference is only 0.11°C. When q_{pen} is neglected, the annual SST with river input is ~0.10°C warmer than without river input. This is opposite to the case when q_{pen} is included. However, the difference in annual SST for the river runs with and without q_{pen} is <0.20°C.

Figure 4d shows the area averaged BLT. The averaged BL is virtually nonexistent from April until September. The deepest BL (~25 m) occurs during the middle of the NEM and vanishes by the end of March. Another shallower BL forms just after the SWM and is only about half as thick. In both cases the BL forms as

water detrains from the ML and the thermocline deepens (Figure 4e). BLs can form as water is detrained from the ML, or as saltier surface waters are subducted under surface waters of the same temperature (e.g., in the western Pacific warm pool region [*Lukas and Lindstrom,* 1991]), creating a halocline in the absence of a thermocline. The BL formation appears to result from ML detrainment, rather than from a subduction process due to cross-frontal advection. In particular, the differences between the BL with and without river input are minimal and so do not argue for a subduction mechanism at salinity fronts as in the western Pacific. The short lifetime of the BL (1-2 months) may be due to the vertical shear between the ML and the underlying water column ($O(1\ e^{-3}\ s^{-1})$ averaged over the bay). The largest difference in BLT occurs in March when the BLT is 1.5 m thicker without river input. With a slightly thicker BL, and a deeper ML, the case without river input has a ML that is better insulated from entrainment cooling. When q_{pen} is neglected, the ML detrainment is larger (i.e., the ML is shallower), and the BL becomes thicker, with thicknesses >30 m during the NEM. Similar to the BL comparison, the SST differences between the two runs are minimal. In all runs, SST does increase during the time when the BL exists. ML temperature can increase when a BL is present because the temperature gradient just below the ML is weak and the halocline is a barrier to vertical mixing. The reasons for the SST increase are examined in section 3.5.

The main thermocline (Figure 4e) exhibits a cycle where it is deepest just near the end of the NEM, after which it shoals until the end of the SWM and then commences deepening again. The thermocline is consistently deeper when q_{pen} and river input are neglected. Since the Ekman pumping is the same for all runs, the differences in stratification and vertical shear, which in turn affect the vertical mixing, are responsible for the changes in thermocline depth. As pointed out by *Han et al.* [2001] along the east coast of India, coastal Kelvin waves driven by fresh water river outflows can change the vertical motion fields near the coast and affect the stratification as well.

3.5. Mixed Layer Heat Budget and SST

The heat flux (q_{net}) into the ocean can be written as

$$q_{\mathrm{net}} = q_{\mathrm{sol}} + q_{\mathrm{sh}} + q_{\mathrm{lh}} + q_{\mathrm{lw}}, \quad (1)$$

where q_{sol} is the flux of shortwave solar radiation, q_{sh} is the sensible heat flux, q_{lh} is the latent heat flux, and q_{lw} is the flux of longwave radiation. All fluxes are positive into the ocean. Much of the absorbed solar heat is lost back to the atmosphere in the form of latent heat and longwave radiation fluxes. Table 2 shows the terms in (1) integrated over an annual cycle. The run with river input nets 5% more heat per unit area averaged over the bay. This is due primarily to less latent heat loss as the SST is slightly cooler with river input. The cooler SST will result in greater heat flux as the atmosphere responds to the cooler SST, but what maintains this cooler SST? There are several processes that could be responsible for the cooling: horizontal advection, penetrative solar radiation loss though the base of the shallower mixed layer (q_{pen}), and vertical entrainment (q_{ent}). Table 2 does show that more heat is lost in the ML because of entrainment cooling and penetrative radiation when river input is included.

In the case where q_{pen} is ignored (Table 3), SSTs are generally only slightly warmer than with q_{pen} because heat loss due to entrainment increases and so dampens the amount of SST rise. The net heat flux difference between the runs with and without river input is negligible in this case.

The relative importance of each of the heat flux terms on changing SST can be examined with the temperature tendency equation for the ML:

$$\frac{\partial T}{\partial t} = -\mathbf{V}\cdot\nabla T + \frac{1}{h\rho C_p}\frac{dq}{dt} = -\mathbf{V}\cdot\nabla T + \frac{1}{h\rho C_p}\left(q_{\mathrm{sol}} + q_{\mathrm{lh}} + q_{\mathrm{sh}} + q_{\mathrm{lw}} + q_{\mathrm{pen}} + q_{\mathrm{ent}}\right), \quad (2)$$

where h is the MLD, and ρ and C_p are the density and specific heat capacity at constant pressure for water, respectively. The convention used for q_{pen} is that it is a negative quantity. Here $\partial T/\partial t$ is computed as a central

Table 2. Heat Flux Integrated Over Annual Cycle

	C1, 10^9 J m^{-2}	R1, 10^9 J m^{-2}	C1-R,1 10^9 J m^{-2}	Average Heat Flux C1-R1, W m^{-2}
$\int q_{\mathrm{sol}}\mathrm{d}t$	6.2637	6.2637	0	0
$\int q_{sh}dt$	0.0022	0.0029	-0.0007	-0.0225
$\int q_{lw}dt$	-1.5359	-1.5408	0.0049	0.1575
$\int q_{lh}dt$	-3.9411	-3.8949	-0.0462	-1.4853
$\int q_{\mathrm{pen}}\mathrm{d}t$	-0.1630	-0.1777	0.0147	0.4726
$\int q_{\mathrm{ent}}\mathrm{d}t$	-0.8603	-0.8980	0.0377	1.2121
$\int q_{\mathrm{net}}\mathrm{d}t$	0.7889	0.8309	-0.0420	-1.3503

Table 3. Heat Flux Integrated Over Annual Cycle[a].

	C2, 10^9 J m^{-2}	R2, 10^9 J m^{-2}	C2-R2, 10^9 J m^{-2}	Average Heat Flux C2-R2, W m^{-2}
$\int q_{\text{sol}}dt$	6.2637	6.2637	0	0
$\int q_{sh}dt$	0.0009	0.0005	0.0004	0.0129
$\int q_{lw}dt$	-1.5309	-1.5256	-0.0053	-0.1704
$\int q_{lh}dt$	-3.9196	-3.9290	0.0094	0.3022
$\int q_{\text{pen}}dt$	0	0	0	0
$\int q_{\text{ent}}dt$	-1.2921	-1.2924	0.0003	0.0096
$\int q_{\text{net}}dt$	0.8141	0.8096	0.0045	0.1447

[a] No penetrative radiation.

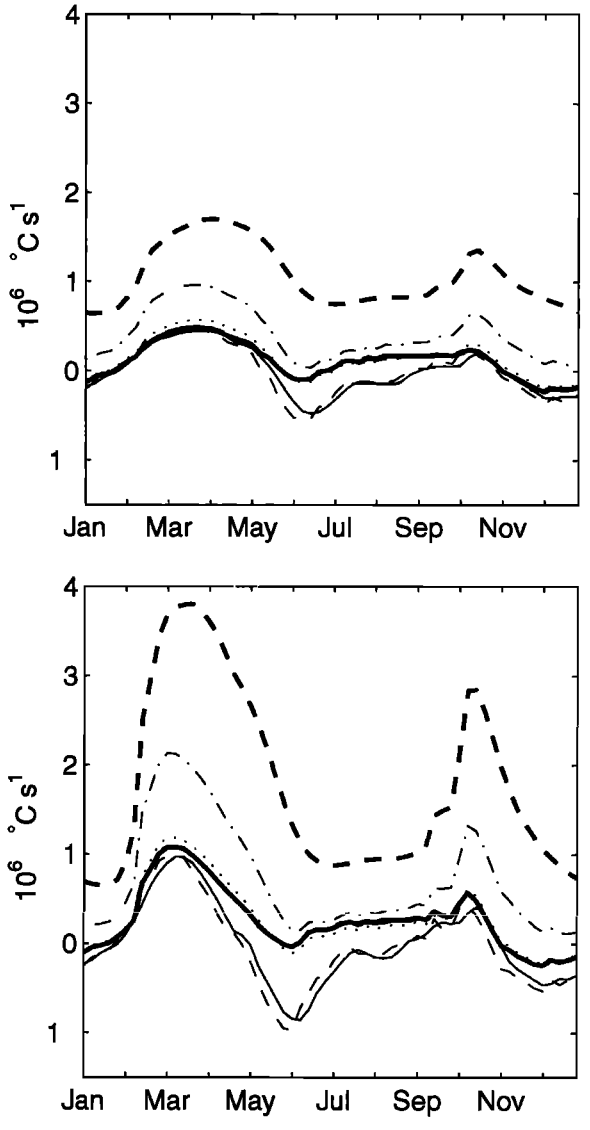

Figure 5. Temperature tendency budget of the ML averaged over the Bay of Bengal interior (see Figure 1 for averaging area): (top) run C1 and (bottom) run C2. The thin line is $\partial T/\partial t$; the thick dashed line is q_{sol}; the dash-dotted line is q_{sol}-q_{LH}; the dotted line is q_{sol}-q_{LH}-q_{LW}; the thick solid line is q_{sol}-q_{LH}-q_{LW}-q_{SH}-q_{pen}; the thin dashed line is q_{sol}-q_{LH}-q_{LW}-q_{SH}-q_{pen}-q_{ent}.

finite difference from the area-averaged SST. Figure 5 shows the annual cycle of the left- and right-hand sides of the tendency equation for the run without river input (without the horizontal advection term) (a) with q_{pen} and (b) without q_{pen}, which illustrates that the balance is nearly one dimensional (a value of $\rho C_p = 4.00 \times 10^6$ J m^{-3} K^{-1} was used). With q_{pen} the balance

$$\frac{\partial T}{\partial t} \sim \frac{q_{\text{net}}}{h\rho C_p} \tag{3}$$

approximately holds, indicating that SST is following the net surface fluxes, except from May until October when river forcing is large and entrainment cooling is important. Without q_{pen} this simpler balance rarely holds, and entrainment cooling is nearly always required in the balance. This illustrates an important result about oceanic adjustment to forcing and the net effect on SST. *Clement et al.* [1996] showed that the tropical Pacific Ocean was capable of regulating SST under anomalous heat flux forcing through cooling of the ML by anomalous upwelling. Clearly, under enhanced buoyancy forcing and ML thinning in the bay, the ML is cooled by enhanced entrainment and a change in stratification. Without a persistent BL SST cannot increase even though the ML shallows with river input.

Figure 6 is a time series of q_{net} for all four runs, averaged over the bay. Integrated over the entire cycle, the biggest difference in net flux is between the river and no river run with q_{pen} (see also Tables 2 and 3). However, the time series exhibits important differences between the runs with and without q_{pen}. First, there are phase differences in q_{net} that are also reflected in the SST time series: q_{net} and SST peak about half a month earlier when q_{pen} is ignored. Thus the ML processes and the interactions between the ML and the atmosphere are affected by q_{pen}. Although the mean net heat flux and SST are very similar between the cases with and without q_{pen}, the phase shift in SST variability and differences in q_{net} would affect the dynamics of the atmosphere in a fully coupled run, even if the amplitude of SST did not change much.

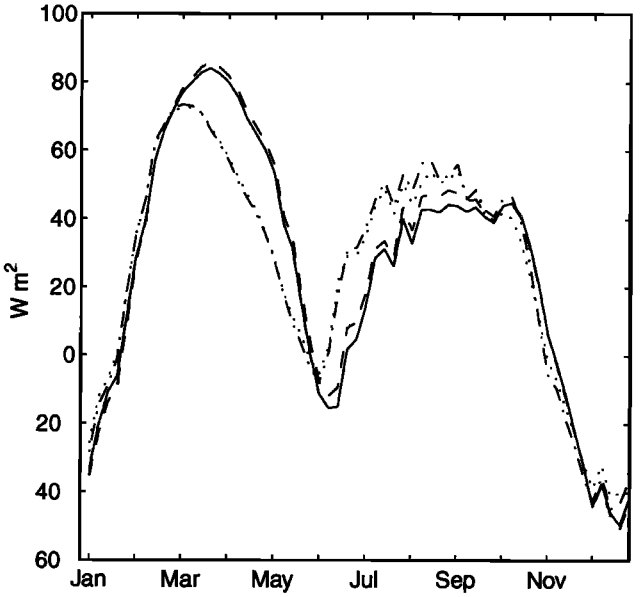

Figure 6. Net heat flux averaged over the Bay of Bengal (see Fig. 1 for averaging area). Dashed (solid) line is run C1 (R1). Dotted (dashed-dot) line is for run C2 (R2).

Although $q_{sol}+q_{pen}$ (i.e., the radiative heating of the ML) is smaller with riverine input (because of shallower MLD), its contribution to temperature tendency is larger than in the control run because of the shallower ML and the exponential-like decay with depth of the shortwave radiation. Similarly, although latent heat loss is smaller with riverine input, it has a greater effect on cooling the shallower ML. Enhanced entrainment cooling in the riverine case is important in balancing the heating due to q_{net}. The thinner ML with riverine input has less entrainment in the mean, so this result is somewhat puzzling at first glance. However, the thinner ML causes entrainment to be more effective at lowering the ML temperature, and it was shown in section 2 that the waters below the ML are cooler with river input. The residual temperature advection is of the order of the sensible heat loss and is much less effective in cooling the ML than any of the other terms.

4. Summary/Discussion

In this paper we have investigated the effects of riverine input into the circulation and hydrography of the Bay of Bengal with emphasis on the effects on the ML in order to determine how the atmosphere, and hence the monsoon, might be affected. Additionally, the effects of q_{pen} were examined. Both rivers and q_{pen} have relatively larger effects on circulation, salinity fields, and subsurface temperature than on SST.

As expected, the inclusion of river input makes the SSS simulation more realistic. Unlike precipitation patterns, which have a broad scale across the bay, riverine input is a concentrated source and creates stronger horizontal density gradients, and hence vertical shear. The result is that the hydrography and circulation of the bay take on a very different character. The subsurface salinity field is also more realistic with a freshwater plume down the center of the bay (90°E) advected from the north and east. The plume is an observed feature of the bay (e.g., VMS96) and is absent in the model runs without riverine input.

River input creates a shallower ML and a shallower thermocline in the Bay of Bengal. The more diffuse thermocline is consistent with stronger vertical mixing in the bay despite the larger buoyancy flux due to river input.

Although the ocean receives more heat with riverine input, slightly cooler SST results because entrainment cooling is more effective, latent heat loss cooling is more effective (despite less latent heat loss), and penetrative radiation is greater, but overall, the SST differences are small. The annual ML is only about 0.1°C colder with river input when averaged over the interior of the bay. One reason that entrainment cooling is more effective in the riverine run (despite the more buoyant ML) is the relatively cooler waters just below the ML. Thus, although the atmosphere adjusts to this cooler SST by increasing the heat flux into the ocean, this added heat is mixed in the vertical and does not increase the temperature of the ML. This contrasts with intuitive expectations of the effects of river input [e.g., *Murtugudde and Busalacchi*, 1999]. The inability of a BL to persist in the Bay also helps to keep SST changes small. Despite the results of *Han et al.*, [2001] that showed a slight average warming in the Bay with riverine input these differences are small (+0.2°C versus −0.2°C) and could change with small perturbations of the heat flux terms.

In some studies [e.g., *Han et al.*, 2001] the water column between the base of the ML and the main thermocline is interpreted as a BL since this layer helps insulate the ML from the strong vertical temperature gradient of the main thermocline. However, the term BL was originally coined to describe a halocline within the upper ocean isothermal layer that not only inhibits vertical mixing, but when it allows mixing, it keeps ML temperature changes minimal because of the weak temperature stratification. Although the water column between the ML and the main thermocline does thicken as the BL forms, the layer remains thicker for several months after the BL disappears (not shown, but see Figure 4). The vertical temperature gradient is not zero beneath the barrier layer and can be important in the heat budget. Thus, although it is appropriate to view the layer between the ML and the main thermocline as an insulator for the ML, it is quite different from a BL and has different consequences for the ML temperature budget and so can influence SST differently.

The neglect of q_{pen} was shown to create a thinner and fresher ML with larger fluctuations of properties about mean values. However, SST was not affected much in the mean. Intra-annual differences in q_{net} with and without q_{pen} may result in dynamical changes in the

atmosphere in a fully coupled model despite the weak changes seen in the SST.

Indian Ocean summer monsoons following El Nino events tend to have heavier than normal rainfall, which would then be followed with heavier than normal river input. *Shukla* [1987] showed that above-average summer monsoon rainfall is followed by negative SST anomalies in the AS and along the mouth of the bay. *Shukla* [1987] speculates that the cooling is due to the stronger winds that accompany high-rainfall monsoons. An alternative hypothesis is that the cooling is due to the higher freshwater input. However, the weak effect of river input on SST in this study and in those of Han99 and *Han et al.*, [2001] lends credence to the former hypothesis that the cooling is due to wind anomalies rather than to freshwater input anomalies.

Acknowledgments. We thank the comments of the two anonymous reviewers for greatly improving the manuscript. R.M. was partially supported by NASA FAS 01-5-26600 for TRMM and NASA NAG 58263 for salinity for which he is extremely grateful. S.H. was supported by NAS NAG 58263. We wish to thank Weiqing Han for graciously providing preprints of her excellent papers.

References

Chen, D., L. M. Rothstein, and A. J. Busalacchi, A hybrid vertical mixing scheme and its application to tropical ocean models, *J. Phys. Oceanogr*, 10, 2156–2179, 1994.

Clement, A. C., R. Seager, M. A. Cane, and S. E. Zebiak, An ocean dynamical thermostat, *J. Clim., 9*, 2190–2196, 1996.

Gent, P., and M. A. Cane, A reduced gravity, primitive equation model of the upper equatorial ocean, *J. Comput. Phys., 81*, 444-480, 1990.

Godfrey, J. S., and E. J. Lindstrom, The heat budget of the equatorial west Pacific surface mixed layer, *J. Geophys. Res., 94*, 8007–8017, 1989.

Han, W., Influence of salinity on dynamics, thermodynamics and mixed layer physics in the Indian Ocean, Ph.D. dissertation, Nova Univ. Fort Lauderdale, Fla., 1999.

Han, W., and J. P. McCrearly Jr., Modeling salinity distribution in the Indian Ocean, *J. Geophys. Res., 106*, 859–878, 2001.

Han, W., J. P. McCrearly Jr., and K. E. Kohler, Influence of P-E and Bay-of-Bengal rivers on dynamics, thermodynamics, and mixed-layer physics in the upper Indian Ocean, *J. Geophys. Res., 106*, 6895-6916, 2001.

Huang, R. X., Real freshwater flux as a natural boundary condition for salinity balance and thermohaline circulation forced by evaporation and precipitation, *J. Phys. Oceanogr., 23*, 2428–2446, 1993.

Kraus, E., and J. Turner, A one-dimensional model of the seasonal thermocline II, *Tellus, 19*, 98–105, 1967.

Levitus, S., Climatological atlas of the world ocean, *NOAA Prof. Pap. 13*, 173 pp., U.S. Govt. Print. Off., Washington, D.C., 1994.

Li, Z., and H. Leighton, Global climatologies of the solar radiation budgets at the surface and in the atmosphere from 5 years of ERBE data, *J. Geophys. Res., 98*, 4919–4930, 1993.

Lukas, R., and E. Lindstrom, The mixed layer of the western equatorial Pacific, *J. Geophys. Res., 96*, 3343–3357, 1991.

McCreary, J. P., Jr, P. K. Kundu, and R. L. Molinari, A numerical investigation of dynamics, thermodynamics and mixed-layer processes in the Indian Ocean, *Prog. Oceanogr., 31*, 181–244, 1993.

Murtugudde, R., and A. J. Busalacchi, Salinity effects in a tropical ocean model, *J. Geophys. Res., 103*, 3283–3300, 1998.

Murtugudde, R., R. Seager, and A. Busalacchi, Simulation of the tropical oceans with an ocean GCM coupled to an atmospheric mixed layer model, *J. Clim., 9*, 1795–1815, 1996.

Murtugudde, R., J. P. McCreary, and A. J. Busalacchi, Oceanic processes associated with anomalous events in the Indian Ocean with relevance to 1997–1998, *J. Geophys. Res., 105*, 3295–3306, 2000.

Oberhuber, J., An atlas based on "COADS" data set, *Rep. 15*, Max-Planck-Inst. für Meteorol., Hamburg, Germany, 1988.

Potemra, J. T., M. E. Luther, and J. J. O'Brien, The seasonal circulation of the upper ocean in the Bay of Bengal, *J. Geophys. Res., 96*, 12,667–12,683, 1991.

Price, J., R. Weller, and R. Pinkel, Diurnal cycle: Observations and models of the upper ocean response to diurnal heating, cooling, and wind mixing, *J. Geophys. Res., 91*, 8411–8427, 1986.

Ramage, C. S., F. R. Miller, and C. Jefferies, *Meteorological Atlas of the International Indian Ocean Expedition,* vol. I, *The Surface Climate of 1963 and 1964*, Nat. Sci. Found., Washington, D.C., 1972.

Rao, R. R., and R. Sivakumar, On the possible mechanisms of the evolution of a mini-warm pool during the pre-summer monsoon season and the genesis of the onset vortex in the south-eastern Arabian Sea, *Q. J. R. Meteorol. Soc., 125*, 787–809, 1999.

Seager, R., and B. Blumenthal, Modeling tropical Pacific sea surface temperature with satellite-derived solar radiative forcing, *J. Clim., 0*, 1–15, 1994.

Seager, R., B. Blumenthal, and Y. Kushnir, An advective atmospheric mixed layer model for ocean modeling purposes: Global simulation of surface heat fluxes, *J. Clim., 8*, 1951–1964, 1995.

Sewell, R. B. S., Temperature and salinity of the surface waters of the Bay of Bengal and Andaman Sea with reference to the Laccadive Sea, *Mem. Asiatic Soc. Bengal, 9*, 131–206, 1929.

Shenoi, S. S. C., D. Shankar, and S. R. Shetye, On the sea surface temperature high in the Lakshadweep Sea, *J. Geophys. Res., 104*, 15,703–15,712, 1999.

Shukla, J., Interannual variability of monsoons, in *Monsoons*, edited by J. S. Fein and P. L. Stephens, pp. 523–548, John Wiley, New York, 1987.

Sprintall, J., and M. Tomczak, Evidence of the barrier layer in the surface layer of the tropics, *J. Geophys. Res., 97*, 7305-7316, 1992.

Varkey, M. J., V. S. N. Murty, and A. Suryanarayana, Physical oceanography of the Bay of Bengal and Andaman Sea, *Oceanogr. Mar. Biol., 34*, 1–70, 1996.

Vinayachandran, P. N., and T. Yamagata, Monsoon response of the sea around Sri Lanka: Generation of thermal domes and anticyclonic vortices, *J. Phys. Oceanogr., 28*, 1946–1960, 1998.

Yu, L., J. J. O'Brien, and J. Yang, On the remote forcing of the circulation in the Bay of Bengal, *J. Geophys. Res., 96*, 20,449–20,454, 1991.

S. D. Howden, Department of Marine Science, University of Southern Mississippi, 1020 Balch Blvd., Stennis Space Center, MS 39529. (stephan.howden@usm.edu)

R. Murtugudde, Earth System Sciences Interdisiplinary Center, CSS Bldg, Room 2201, University of Maryland, College Park, MD 20742. (ragu@vinsanto.essic.umd.edu)

(Received September 25, 2000; revised March 20, 2001; accepted March 22, 2001.)